JOURNAL OF PROPULSION AND POWER
Vol. 25, No. 3, May–June 2009

Predicting Hybrid Propellant Regression Rate Using Response Surfaces

Robert A. Frederick Jr.*
University of Alabama in Huntsville, Huntsville, Alabama 35899
and
J. Joshua Whitehead†
ATK Launch Systems, NASA Marshall Space Flight Center, Alabama 35812

DOI: 10.2514/1.14418

Applied mixture theory allows for estimation of propellant characteristics (such as regression rate or specific impulse) over an extended range of formulations from a limited number of tests. A mixed-oxidizer hybrid system was tested using fuel formulations of 25–30% ammonium perchlorate, 0–5% iron oxide, and 70–75% hydroxyl-terminated polybutadiene fired with gaseous oxygen. Through application of a reduced form of the cubic response equation, functional relationships were developed that correlate fuel composition to regression rate in the form of a three-dimensional response surface. The maximum regression rate was then estimated to occur at approximately 2% iron oxide and 27.5% ammonium perchlorate based on the response surface developed from experimental results at an oxidizer flux of 0.3 $\mathrm{lb}_m/\mathrm{in}^2 \cdot \mathrm{s}$ (0.211 $\mathrm{kg}/\mathrm{m}^2 \cdot \mathrm{s}$) and a chamber pressure of 350 psia (2.41 MPa).

Nomenclature

a	=	regression rate law coefficient
a_{ij}	=	response surface correlation coefficients
C_a	=	response surface correlation coefficient for regression rate law coefficient
C_m	=	response surface correlation coefficient for oxidizer flux exponent
C_n	=	response surface correlation coefficient for pressure exponent
G_{ox}	=	oxidizer mass flux ($\mathrm{lb}_m/\mathrm{in}^2 \cdot \mathrm{s}$)
m	=	oxidizer mass flux exponent in regression rate law
n	=	pressure exponent in regression rate law
P	=	chamber pressure, psi
$\dot{r}$	=	regression rate of propellant grain, in/s
x_i	=	independent (mixture) variables
y	=	dependent (response) variable
η_i	=	normalized mixture variables

Introduction

THOUGH hybrid rockets offer a number of benefits in terms of safety and mission flexibility, the fuel grains used in hybrid systems typically exhibit low regression rates. This results in less attractive performance attributes compared to competitive solid and liquid propulsion systems. An increase in the regression rate of the hybrid fuel will improve the viability of this system as a competitive option in the marketplace. Advances in fuel formulation are targeted in this study as a method to increase the regression rate in a hybrid rocket propulsion system [1]. Applied mixture theory is used as a tool to construct a minimum number of experimental tests necessary to provide predictive capability for estimation of regression rate across the operational and mixture variable spaces. Mixture-dependent coefficients are derived as a tool for subsequent generation of response surfaces to provide for estimation of mixed-oxidizer hybrid (MOH) regression rates within the domain of interest.

Mixture theory is an applicable design tool for determination of the required matrix of fuel grain formulations [2]. Through rigorous application of mixture theory, a response surface for the proposed propellant components can be determined from a minimal number of tests, as provided by applied mixture theory [2]. Kurotori proposed a cubic expression that relates a desired response function to its three mixture components as given by Eq. (1) [3]:

$$y = a_1 \cdot x_1 + a_2 \cdot x_2 + a_3 \cdot x_3 + a_{12} \cdot x_1 \cdot x_2 + a_{13} \cdot x_1 \cdot x_3 + a_{23} \cdot x_2 \cdot x_3 + a_{123} \cdot x_1 \cdot x_2 \cdot x_3 \quad (1)$$

The coefficients a_1, a_2, and so on are correlation coefficients that relate the desired response function to the various compositional effects of the mixture. Each x value represents a mass fraction of a specific mixture component. Hydroxyl-terminated polybutadiene (HTPB), ammonium perchlorate (AP), and iron oxide (Fe_2O_3, additive or catalyst) mass fractions are denoted as x_1, x_2, and x_3, respectively.

Independent variables for a ternary mixture (containing three components) can be plotted in three dimensions using a Cartesian coordinate system. When considering all possible mixtures, this factor space is a cube of sides ranging from 0 to 100% of each mixture component. However, for experimental studies, this factor space must be effectively fixed so that a minimum number of tests can be performed, resulting in predictive models that are applicable over a large range of data [4]. Geometrically, this forces all three sides of the triangular region bound by the new factor space to be of identical lengths (or mixture percentages). The factor space for the mixed variables considered cannot range over all possible values of each component, but must be fixed to a triangular region as dictated by the requirement that all mass fractions must sum to one. Figure 1 is a pictorial representation of these geometrical considerations of factor space for experimental mixture studies.

In traditional mixture theory, ranges from 0 to 100% are considered for testing. However, in the manufacture of propellant grains, individual components of the mixture seldom vary over such a large range. In such cases, the factor space is constrained over a region of identical geometry but smaller ranges are applied to each of the edges of the triangular region of the factor space. This new range is determined by setting applicable upper or lower bounds for each of

Presented as Paper 3545 at the 41st AIAA/ASME/SAE/ASEE Joint Propulsion Conference & Exhibit, Tucson, AZ, 10–13 July 2005; received 25 October 2007; revision received 26 June 2008; accepted for publication 5 October 2008.

*Interim Director, Propulsion Research Center, 5000 Technology Drive. Associate Fellow AIAA.
†Engineer.

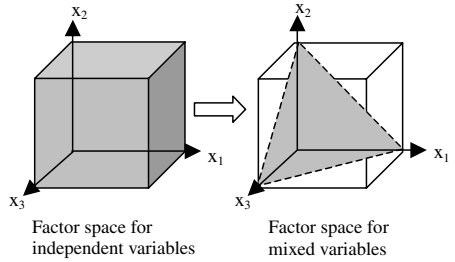

Fig. 1 Mixture component ranges of an unfixed and fixed factor space.

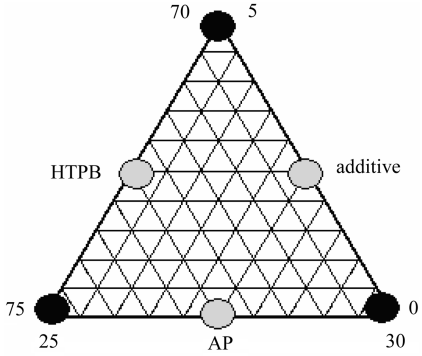

Fig. 2 Ternary mixture diagram for assessment of experimental MOH concept.

the mixture components and assessing an appropriate range of study that is compatible with all components [3].

When the ranges of applicability for the mixed-oxidizer hybrid concept are applied, a ternary diagram for the fuel (HTPB), oxidizer (AP), and additive or catalyst (iron oxide) is created [5]. The ternary mixture diagram used in this study is shown in Fig. 2. A range of 5% variation in mass fraction of each component was chosen to allow a range of catalyst mixture fraction, including a zero level, but not significantly exceeding typical industrial applications, while also allowing a sufficiently large variation in oxidizer component contribution.

A regression rate model was proposed to include pressure and oxidizer flux effects and is given in Eq. (2) [6]. This model incorporates sensitivity to oxidizer flux, as is typically applied to hybrid rocket motor regression rate models, and motor chamber pressure as used in solid rocket motor regression rate models:

$$\dot{r} = aG_{\text{ox}}^{m}P^{n} \tag{2}$$

A testing matrix was then designed to assess the impact of these two operational parameters on the regression rate of each mixed-oxidizer hybrid propellant formulation. To determine both pressure and oxidizer flux effects, a total of three tests were required for each propellant formulation given in Fig. 2. A summary of the operational conditions targeted during experimental testing at each of the six propellant mixture formulations is given in Table 1. Additional discussion of the empirical methods and conduct of experimentation is outlined in [6].

The results of this study show that mathematical tools such as response surfaces and applied mixture theory can be used to formulate experiments that provide a maximum range of applicability of results with a minimum number of tests. Experimental data generated from target experiments were used to develop response surface coefficients for predictive modeling of the maximum regression rate within the bounds of the design mixture space and operational variable limits. The results demonstrate how to maximize the propellant burning rate within the bounds of the experiments conducted.

Table 1 Summary of target operational conditions during testing [6]

	G_{ox}, kg/m$^2 \cdot$ s	P, MPa
Low G_{ox}, low P	0.075	2.07
High G_{ox}, low P	0.280	2.07
Low G_{ox}, high P	0.075	4.14

Approach

Summary of Ballistic Data

Three experiments were performed using various operating conditions (oxidizer flux and chamber pressure) for all the fuel formulations depicted in Fig. 2. These included a low oxidizer flux setting at low chamber pressure, low oxidizer flux at high chamber pressure, and high oxidizer flux at low chamber pressure. Equation (2) was applied to the experimental data to provide a set of equations that yield values of the regression rate coefficient a, flux exponent m, and pressure exponent n for each fuel formulation [6]. The results of this data reduction are given in Table 2.

Response Surface Methodology

The cubic form of a response function given in Eq. (1) can be reduced to a quadratic form by neglecting the final (cubic) term. This approach is applicable to most problems and is typically used to allow for a solvable set of equations [3]. The assumption is an application of the Sparsity of Effects Principle, which asserts that main effects and two-way mixture interactions dominate within mixture systems and higher-order interaction terms can be neglected [7]. This revised formula as given in Eq. (3) is used to develop response surface coefficients for the experimental data:

$$y = a_1 \cdot x_1 + a_2 \cdot x_2 + a_3 \cdot x_3 + a_{12} \cdot x_1 \cdot x_2 + a_{13} \cdot x_1 \cdot x_3 + a_{23} \cdot x_2 \cdot x_3 \tag{3}$$

Equation (3) can be restated in terms of each of the regression rate law parameters, such that each parameter is expressed as a function of the mixture composition of the hybrid fuel [Eqs. (4–6)]:

$$a(x_1, x_2, x_3) = Ca_1 \cdot x_1 + Ca_2 \cdot x_2 + Ca_3 \cdot x_3 + Ca_{12} \cdot x_1 \cdot x_2 + Ca_{13} \cdot x_1 \cdot x_3 + Ca_{23} \cdot x_2 \cdot x_3 \tag{4}$$

$$m(x_1, x_2, x_3) = Cm_1 \cdot x_1 + Cm_2 \cdot x_2 + Cm_3 \cdot x_3 + Cm_{12} \cdot x_1 \cdot x_2 + Cm_{13} \cdot x_1 \cdot x_3 + Cm_{23} \cdot x_2 \cdot x_3 \tag{5}$$

$$n(x_1, x_2, x_3) = Cn_1 \cdot x_1 + Cn_2 \cdot x_2 + Cn_3 \cdot x_3 + Cn_{12} \cdot x_1 \cdot x_2 + Cn_{13} \cdot x_1 \cdot x_3 + Cn_{23} \cdot x_2 \cdot x_3 \tag{6}$$

These equations are solved using the experimental data in Table 2 to give values of the response surface coefficient for each regression rate parameter. Equation (2) can be further expanded by substitution of Eqs. (4–6), yielding a functional relationship between hybrid fuel regression rate and oxidizer flux, chamber pressure, and mixed-oxidizer hybrid fuel composition [Eq. (7)]:

$$\dot{r}(x_1, x_2, x_3, G_{\text{ox}}, P) = a(x_1, x_2, x_3) \cdot G_{\text{ox}}^{m(x_1, x_2, x_3)} \cdot P^{n(x_1, x_2, x_3)} \tag{7}$$

Table 2 Summary of experimental regression rate law parameters by composition

x_1	x_2	x_3	a	m	n
0.725	0.275	0.000	0.021	0.157	0.187
0.725	0.250	0.025	0.070	0.094	0.064
0.750	0.250	0.000	0.033	0.355	0.188
0.700	0.300	0.000	0.038	0.280	0.137
0.700	0.275	0.025	0.187	0.240	0.015
0.700	0.250	0.050	0.082	0.434	0.108

Table 3 Response surface coefficients for regression rate law parameters

Coefficient	$i = a$	$i = m$	$i = n$
Ci_1	1.748	19.990	−2.497
Ci_2	12.288	134.050	−21.157
Ci_3	−67.872	340.730	142.783
Ci_{12}	−23.200	−256.800	39.200
Ci_{13}	20.000	−480.800	−134.400
Ci_{23}	203.200	−187.200	−172.000

Results and Discussion

Response Surface Coefficients

The response surface coefficients for the regression rate coefficient, flux exponent, and pressure exponent are calculated using experimental data and Eqs. (4–6). A set of six equations with six unknowns is solved simultaneously for each parameter (a, m, and n). Values obtained for these parameters are presented in Table 3. Note that, due to the arrangement of six mixture treatments as shown in Fig. 3 and the applied response surface in quadratic form as given by Eq. (3), the six response surface coefficients provide exact fit of regression rate results at the experimental anchor points. Regression rates are estimated by interpolation within the experimental mixture space using the selected response surface form and calculated coefficients.

Benchmark Burning Rates

All possible regression rates for the experimentally bounded ranges shown in Fig. 2 are now easily compared by setting operating conditions and plotting the response function (regression rate) in terms of mixed-oxidizer hybrid propellant composition using the functional relationship depicted in Eq. (7) along with the response surface coefficients in Table 3. Because the sum of individual mass fractions of the components must equal unity, only two mixture components need to be specified to fix the state of the system. Thus, the response of regression rate can be plotted in a three-dimensional space as a function of two mixture component mass fractions at fixed oxidizer flux and chamber pressure. Ternary diagrams, as used in Figs. 3 and 4, are also a useful means of representing response surfaces for regression rate as a function of mixture components [8]. Response surfaces are presented in Figs. 3–6 at a fixed chamber pressure and oxidizer flux with varying mixture compositions. The chosen oxidizer flux and chamber pressure are bounded by the experimentally observed test conditions. Note that the response surface as plotted in Figs. 3–6 represents estimated or interpolated values of regression rate within the mixture space defined by Fig. 2 as observed during experimental results.

Trends suggest that an initial and rapid improvement in regression rate occurs upon addition of burning rate catalyst. However, further addition of catalyst above 2% leads to decreased regression rate. A similar trend was noted for addition of AP, which showed a peak improvement in regression rate at approximately 27.5%.

When mixture component variables are recast in the form of normalized values, relative contributions of the burn rate coefficients and exponents and their impact on the burn rate can be assessed for a fixed oxidizer flux and chamber pressure. Mixture components x_1, x_2, and x_3 are recast as η_1, η_2, and η_3 by normalizing each variable to range from -1 to $+1$ in magnitude. The burn rates resulting from application of response surface coefficients at a fixed set of operating conditions are summarized in Table 4.

The highest observed burned rate for the mixed-oxidizer hybrid system is observed at the mixture composition $\boldsymbol{\eta}_i = [-1, 0, 0]$ or

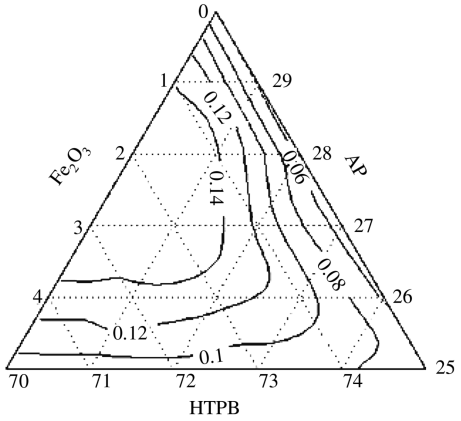

Fig. 3 Ternary regression rate line contour plot (in./s) for G_{ox} = 0.3 $lb_m/in.^2 \cdot s$ (0.211 $kg/m^2 \cdot s$) and P = 350 psi (2.41 MPa).

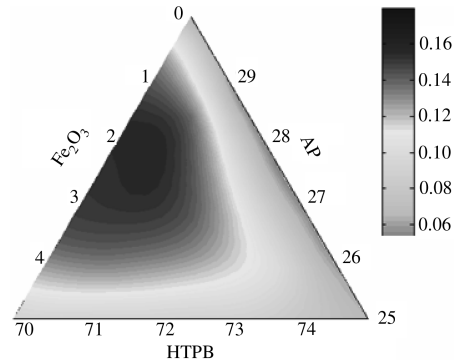

Fig. 4 Ternary regression rate response surface (in./s) for G_{ox} = 0.3 $lb_m/in.^2 \cdot s$ (0.211 $kg/m^2 \cdot s$) and P = 350 psi (2.41 MPa).

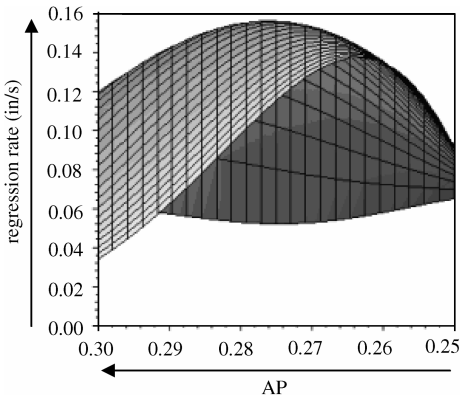

Fig. 5 Pseudo-three-dimensional plot of regression rate vs AP mass fraction for G_{ox} = 0.3 $lb_m/in.^2 \cdot s$ (0.211 $kg/m^2 \cdot s$) and P = 350 psi (2.41 MPa).

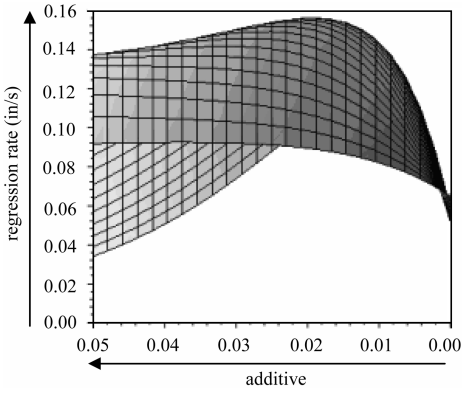

Fig. 6 Pseudo-three-dimensional plot of regression rate vs additive mass fraction for G_{ox} = 0.3 $lb_m/in.^2 \cdot s$ (0.211 $kg/m^2 \cdot s$) and P = 350 psi (2.41 MPa).

Table 4 Burn rates for $G_{ox} = 0.3$ lb$_m$/in.$^2 \cdot$ s (0.211 kg/m$^2 \cdot$ s) and $P = 350$ psi (2.41 MPa)

η_1	η_2	η_3	a	m	n	Burn rate, in./s
0	0	−1	0.021	0.157	0.187	0.052
−1	1	−1	0.038	0.280	0.137	0.061
1	−1	−1	0.033	0.355	0.188	0.065
0	−1	0	0.070	0.094	0.064	0.091
−1	−1	1	0.082	0.434	0.108	0.092
−1	0	0	0.187	0.240	0.015	0.153

when AP and additive mass fractions are 27.5% and 2.5%, respectively.

These observed responses are supported notionally by the physics of the combustion processes associated with the mixed-oxidizer hybrid motor. Solid rocket motor catalysts such as iron oxide provide augmentation of burn rate by activation of additional sites for oxidizer decomposition in the fuel grain. At catalyst levels beyond that necessary to ensure adequate oxidizer decomposition at the flame front, the excess catalyst content becomes inert loading incumbent in the fuel grain. Thus, at higher catalyst levels (above 2% mass fraction) the burning rate augmentation caused by addition of the catalyst is offset by burning rate losses due to lower fuel and oxidizer availability in the grain. Oxidizer is also available to support combustion from two sources in the mixed-oxidizer hybrid rocket design, including 25–30% AP mass fraction in the fuel grain (depending on the mixture assessed) and gaseous oxygen injected into the combustion chamber. Experimental results suggest that adequate oxidizer is available from the combined solid and gaseous sources at the considered operating conditions with an AP constituent of 27.5% by mass. Above this level, additional oxidizer in the grain reduces available fuel (HTPB) content, which could lead to a decrease in burn rate. Further studies of oxidizer-to-fuel ratio during experimental operations are needed to quantify these qualitative assessments.

Conclusions

Use of response surfaces in conjunction with applied mixture theory has unique applications in optimization of propulsion systems. The results of this study show that a minimum number of tests specified by mixture theory can be used effectively to determine a composition that will result in improved regression rates. A regression rate model combining aspects of hybrid and solid rocket motor burning rate laws was assumed, and coefficients and exponents for the functional terms in the relationship were derived in the form of response surface coefficients. These coefficients, when applied to the regression rate law at fixed operating conditions, provide comprehensive coverage of the mixture space bounded by the ternary mixture design. Estimates of regression rate for various fuel grain formulations were evaluated at different operating conditions in an effort to determine optimum mixture and operating conditions for maximum regression rate. A relative maximum for one set of operating conditions intermediate within the range of experimental tests was found at an AP level of 27.5% and an additive level of approximately 2% by mass, which is qualitatively supported by the combustion mechanics of the mixed-oxidizer hybrid design.

Further optimization and uncertainty analysis studies are planned. Additional design of experiment scenarios may also be sought which could benefit from the use of response surfaces to relate system conditions to desired system outcomes. Further review of the application of derived response surfaces to propulsion system design and optimization should also be considered. Optimization for desired system properties is possible through use of these derived response surfaces and application of appropriate constraints for the desired system response or responses. Optimization efforts including detailed uncertainty analysis are planned to build upon the response surface methodology discussed in this article.

References

[1] Frederick, R. A., Knox, L. R., and Moser, M. D., "Mixed Hybrid Propellants," AIAA Paper 2003-4745, July 2003.

[2] Cornell, J. A., "Experiments with Mixtures: A Review," *Technometrics*, Vol. 15, No. 3, 1973, pp. 437–455. doi:10.2307/1266850

[3] Kurotori, I. S., "Experiments with Mixtures of Components Having Lower Bounds," *Industrial Quality Control*, Vol. 22, No. 11, May 1966, pp. 592–596.

[4] Snee, R. D., "Design and Analysis of Mixture Experiments," *Journal of Quality Technology*, Vol. 3, No. 4, Oct. 1971, pp. 159–169.

[5] Frederick, R. A., Jr., Knox, L. R., Moser, M. D., and Whitehead, J. J., "Ballistic Properties of Mixed Hybrid Propellants," AIAA Paper 2004-3824, July 2004.

[6] Frederick, R. A., Jr., Knox, L. R., Moser, M. D., and Whitehead, J. J., "Regression Rates Study of Mixed Hybrid Propellants," *Journal of Propulsion and Power*, Vol. 23, No. 1, Jan.–Feb. 2007, pp. 175–180. doi:10.2514/1.14327

[7] Montgomery, D. C., *Design and Analysis of Experiments*, 6th ed., Wiley, Hoboken, NJ, 2005.

[8] Sandrock, C., "Ternplot," *Matlab Central File Exchange*, Aug. 2002, http://www.mathworks.com.

S. Son
Associate Editor